Surface-acoustic-wave properties of MgO-doped LiNbO3 single crystals measured by line-focus-beam acoustic microscopy

doi: 10.1063/1.370597

Surface-acoustic-wave properties of MgO-doped $LiNbO_3$ single crystals measured by line-focus-beam acoustic microscopy

J. Kushibiki, T. Kobayashi, and H. Ishiji
Department of Electrical Engineering, Tohoku University, Sendai 980-8579, Japan

C. K. Jen
Industrial Material Institute, National Research Council, Boucherville, Quebec, Canada J4B 6Y4

(Received 5 January 1999; accepted for publication 22 February 1999)

Basic acoustic properties of five MgO-doped $LiNbO_3$ rectangular parallelpiped specimens, having *X*-, *Y*-, and *Z*-cut planes, with different MgO dopant concentrations ranging from 0 to 13 mol % are investigated by line-focus-beam acoustic microscopy. The investigation is conducted to characterize the optical-use MgO:$LiNbO_3$ crystals and wafers and to establish large-diameter crystal growth conditions. Leaky-surface-acoustic-wave (LSAW) velocities are measured on each crystalline plane of each specimen as a function of the wave propagation direction and are compared with the measured chemical composition ratios of Mg/Li/Nb, densities, and lattice constants. It is shown that, as the dopant concentrations increase in the experimental composition region, the LSAW velocities increase almost linearly for all the surfaces and all the propagation directions. The LSAW velocities are linearly proportional to the lattice constants, but inversely proportional to the densities. © *1999 American Institute of Physics.* [S0021-8979(99)01511-X]

I. INTRODUCTION

$LiNbO_3$[1–4] is a very attractive ferroelectric material used for optoelectronic and surface-acoustic-wave (SAW) devices. For optical use, $LiNbO_3$ must be doped with MgO, ZnO, and In_2O_3 to suppress optical damage.[5–8] MgO-doped $LiNbO_3$ crystals have been extensively investigated to develop large-diameter crystals with optically homogeneous properties.[9–12] The technology for analyzing and evaluating crystals is of fundamental importance in establishing the growth conditions for high-quality crystals, for which crystalline perfection and compositional homogeneity must be evaluated precisely. X-ray analysis, differential temperature analysis, inductively coupled plasma analysis, electron probe microanalysis, and other methods are usually employed for evaluation. However, these evaluation techniques still have the following problems: insufficient accuracy, unavoidable destruction of samples, very long examination time, and very high cost. Although such conventional evaluation techniques have been improved, a new analytical and evaluation technique should still be developed to perform nondestructive, noncontacting inspections. Line-focus-beam (LFB) acoustic microscopy[13] has been considered one of the more promising methods to meet such requirements.

LFB acoustic microscopy enables very accurate measurements of the propagation properties, especially phase velocity, of leaky-surface-acoustic-waves (LSAWs) excited on the boundary between a solid specimen and water as an acoustic couplant.[13] We have applied LFB acoustic microscopy to $LiNbO_3$ crystals for SAW-device use to determine the relationship of the LSAW velocities to the chemical composition ratios of Li/Nb and densities. The results have proven that changes in chemical composition and density are very easily detectable elastically as variations in LSAW velocity.[14] Furthermore, this ultrasonic method has been applied to MgO: $LiNbO_3$ crystals, and the sensitivity and resolution for other chemical and physical properties, such as chemical composition, lattice constant, refractive index, Curie temperature, and density, have been shown to be much greater than those of conventional methods.[15]

This article seeks to collect basic data on the acoustic properties of LSAW velocities, related directly to the chemical compositions, before applying the method to the practical problems of characterizing MgO-doped $LiNbO_3$ crystals and wafers and establishing large-diameter crystal growth conditions. Several MgO: $LiNbO_3$ crystals specially grown with different MgO dopant concentrations ranging from 0 to 13 mol % are prepared. LSAW velocities are measured for three basic crystal surfaces, *X*-, *Y*-, and *Z*-cut planes, of each specimen as a function of the wave propagation direction. The LSAW velocities are discussed in relation to the chemical composition ratios of Li/Nb/Mg, densities, and lattice constants.

II. LFB SYSTEM

The method and system for LFB acoustic microscopy have been described in detail elsewhere.[13,16] With this system, LSAWs are excited and propagated on the water-loaded sample surface. The propagation characteristics, viz., phase velocity and propagation attenuation, can be determined by analyzing *V(z)* curves, which are the transducer outputs recorded by changing the *z* distance between an LFB ultrasonic device and a specimen. The material is evaluated with the phase velocities in this study. Figure 1 shows the typical *V(z)* curve measured for the *Z*-cut, *Y*-propagating, undoped $LiNbO_3$ at 225 MHz and the final results analyzed by a fast Fourier transform (FFT). According to the *V(z)* curve analy-

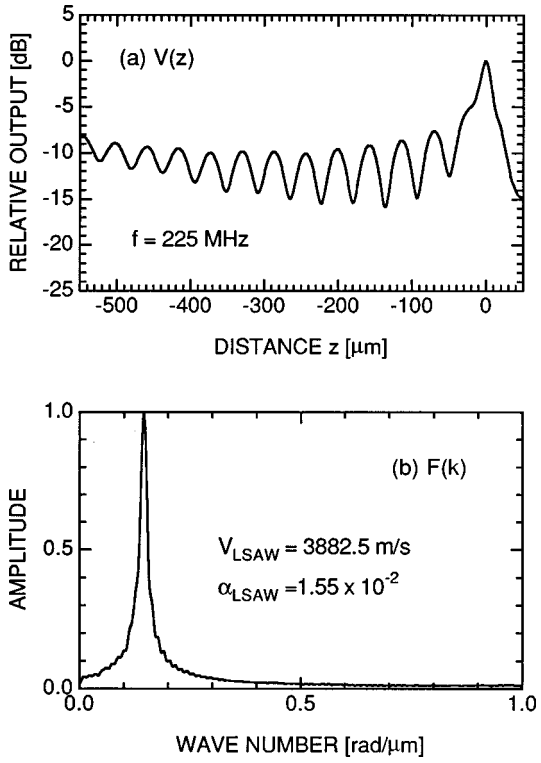

FIG. 1. Typical *V(z)* curve measured for a *Z*-cut, *Y*-propagating, undoped $LiNbO_3$ specimens at 225 MHz and final spectral distribution analyzed by FFT for the *V(z)* curve shown above.

sis procedure[13] and using the physical properties of distilled water as reference, the phase velocities of LSAWs, V_{LSAW}, can be obtained from the oscillation interval Δz in the *V(z)* curve as

$$V_{\mathrm{LSAW}}=\frac{V_W}{\sqrt{1-(1-V_W/2f\Delta z)}}, \tag{1}$$

where V_W is the longitudinal velocity of water, and f is the ultrasonic frequency. The system measured LSAW velocity with a relative accuracy exceeding $\pm 0.005\%$ for a single measurement and $\pm 0.01\%$ over the entire scanning area of 75×75 mm.[16]

III. SAMPLES

Five rectangular parallelpiped specimens, Nos. 1–5, of about $8\times 9\times 10$ mm were prepared from MgO:$LiNbO_3$ crystals with different Mg/Li/Nb ratios at the Institute of Acoustics, Beijing, People's Republic of China. Each surface is shaped into *X*-, *Y*-, and *Z*-cut planes. The composition of each specimen was determined by inductively coupled plasma spectrometry, as shown in Table I. The densities were measured by the Archimedes method, and the lattice constants of *a* and *c*, by x-ray diffractometry using the Bond method for comparison with the LSAW velocities obtained in the following experiments. Table I also presents the data measured for the 75-mm diameter *Z*-cut $LiNbO_3$ wafers with 0- and 5-mol % MgO dopants, commercially available from Yamaju Ceramics Co., Seto, Japan. It can be seen that, in general, as the MgO concentration increases in the experimental range, resulting in the subsequently different ratios of Mg/Li/Nb, the density decreases monotonically and the lattice constants *a* and *c* increase almost linearly, as reported by Grabmaier and Otto.[10]

IV. RESULTS AND DISCUSSIONS

First, the angular dependences of the LSAW velocities for the five specimens were measured at the center of the specimen surfaces of *X*, *Y*, and *Z* crystalline planes at 225 MHz. Figure 2 shows the results for each surface, in which the velocities vary significantly with the propagation direction, reflecting the crystal symmetry. The propagation directions of 0° and 90° for the *X*-cut planes in Fig. 2(a) correspond to the *Y* and *Z* axes, respectively; those for the *Y*-cut planes in Fig. 2(b), to the *X* and *Z* axes; and those for the *Z*-cut planes in Fig. 2(c), to the *X* and *Y* axes. As the MgO concentrations increase, the LSAW velocities increase almost linearly on each surface and for all propagation directions. Figure 3 shows the increasing rates of the LSAW velocities for all directions, calculated from the maximum differences between samples No. 1 and No. 5 along each propagation direction in Fig. 2. The increasing rates depend remarkably upon the crystalline surfaces and propagation directions. The rates on the *X*- and *Y*-cut planes are generally larger around the *Z*-axis propagation directions than those on the *Z*-cut planes, especially the largest around the propagation direction of 120° for *X*-cut planes. On the *Z*-cut planes, smaller variations of the rates are observed, although the rates exhibit minima around the equivalent *Y*-axis directions.

In the above, the full information of the LSAW velocity variations for all propagation directions on the three basic crystalline planes (*X*-, *Y*-, and *Z*-cut planes) was obtained. When applying the system to evaluate the crystal or wafer quality and to improve the crystal growth conditions, the

TABLE I. MgO: $LiNbO_3$ specimens and their chemical compositions, densities, and lattice constants.

Sample No.	Composition (mol %)			Density (kg/m^3)	Lattice constant (Å)	
	MgO	Li_2O	Nb_2O_5		*a*	*c*
1	2.45	47.01	50.54	4639	5.1504	13.8670
2	6.46	44.29	49.25	4632	5.1517	13.8720
3	9.43	43.28	47.28	4620	5.1526	13.8767
4	11.97	41.57	46.46	4609	5.1537	13.8812
5	12.62	41.94	45.44	4605	5.1537	13.8810
6	0	48.42	51.58	4643.0	···	13.8658
7	4.89	45.84	49.27	4638.2	···	13.8704

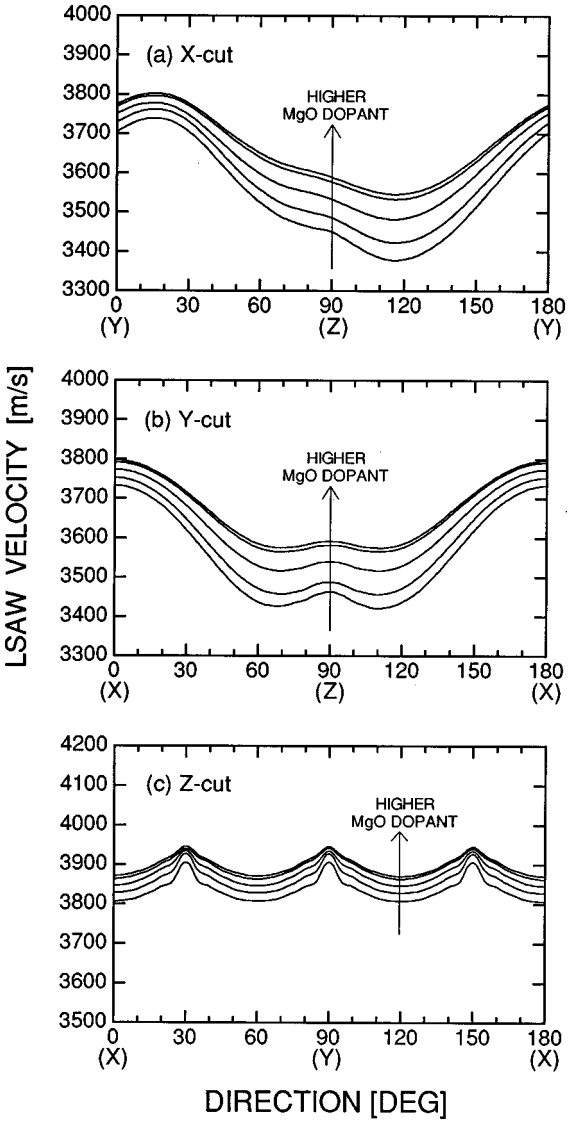

FIG. 2. Angular dependences of LSAW velocities on *X*-, *Y*-, and *Z*-cut planes of MgO:$LiNbO_3$ as a function of MgO dopant concentration.

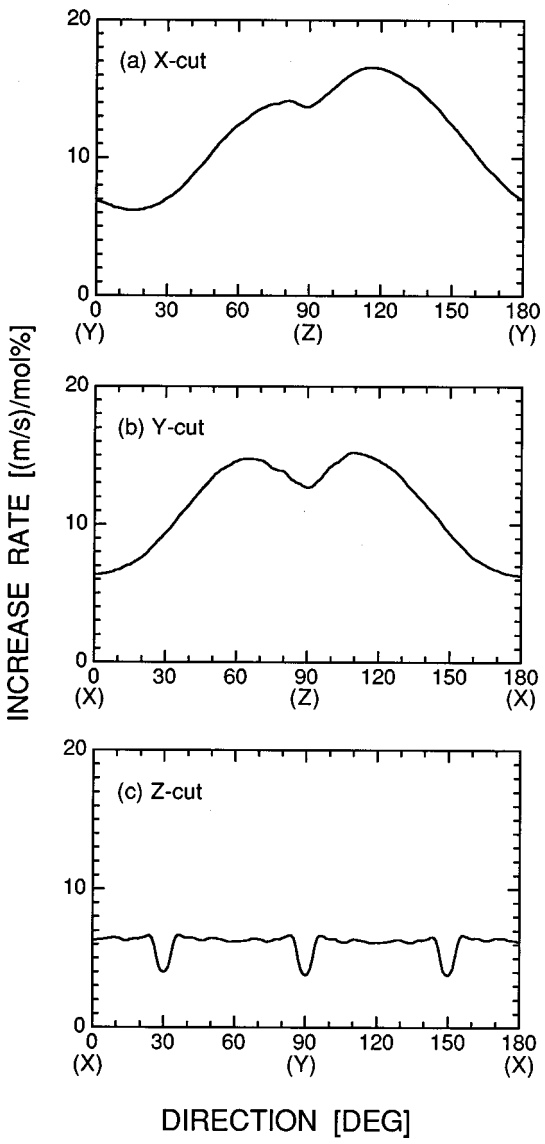

FIG. 3. Angular dependences of increasing rates of LSAW velocities to MgO dopant concentration on *X*-, *Y*-, and *Z*-cut planes of MgO: $LiNbO_3$.

propagation directions should fundamentally be selected along the principal axes on each basic plane. However, on the *X*-cut planes, the *Y*- and *Z*-axis propagation directions might not be suitable for accurate measurements, as the power flow angles of LSAWs are not equal to zero. In this case, the 16°*Y* and 117°*Y* directions, where the power flow angles become zero, might be better, as seen in Fig. 2. On the *Y*-cut planes, the *X* and *Z* directions can be utilized for measurements, while, on the *Z*-cut planes, the *X* and *Y* directions can be utilized. It is therefore meaningful to graph and discuss the interrelations among the chemical compositions, LSAW velocities, densities, and lattice constants for these six directions on the planes.

Figure 4 shows the relationship between the MgO concentrations and the LSAW velocities, including the data for the undoped and 5-mol % MgO-doped, *Z*-cut $LiNbO_3$wafers. The solid lines were obtained by linear approximation using the lest squares method. The LSAW velocities increase monotonically with the MgO concentrations in the experimental range. The velocities for the undoped specimen are relatively separated from the solid lines. It can be deduced that the velocity could increase with the higher increasing rates in the more lightly doped region. The relations of the LSAW velocities to the densities and the lattice constants *a* and *c* are presented in Figs. 5, 6, and 7. From these three figures, we can completely understand the interrelations among the MgO concentrations, LSAW velocities, densities, and lattice constants. The LSAW velocities and lattice constants are linearly proportional to the MgO concentrations, and the densities are inversely proportional to the LSAW velocities. Through the velocity measurements by the LFB system, we can obtain information of some changes of chemical composition, density, and some other physical constants related to the compositional changes.[15] That increasing MgO dopants causes the densities to decrease can be easily understood from the fact that Mg atoms with an atomic weight of 24.312 replace Li atoms with an atomic weight of 6.939 and Nb atoms with an atomic weight of 92.906, resulting in the ratios of Mg/Li/Nb shown in Table I. The LSAW

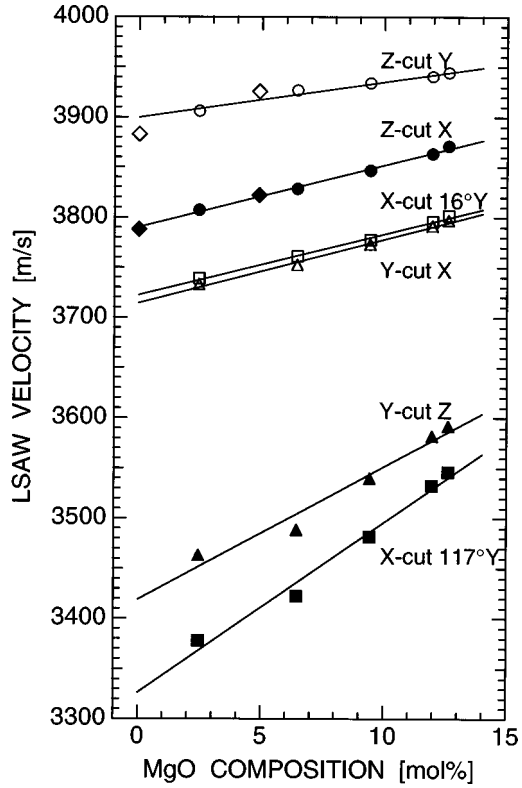

FIG. 4. LSAW velocities in typical propagation directions as a function of MgO concentration. ◇ and ◆: data for samples No. 6 and No. 7.

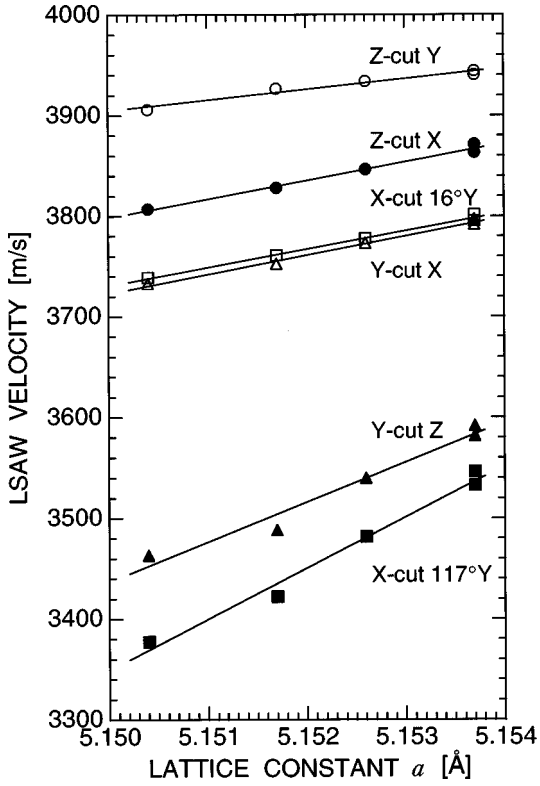

FIG. 6. LSAW velocities in typical propagation directions as a function of lattice constant *a*.

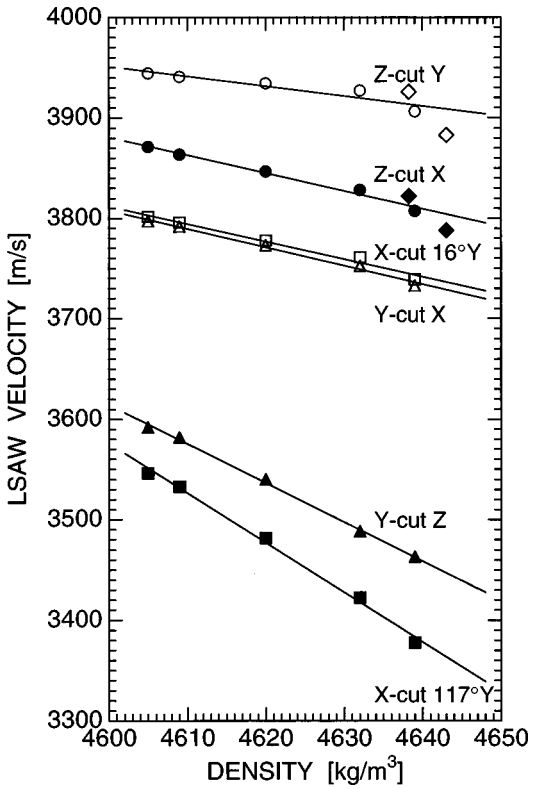

FIG. 5. LSAW velocities in typical propagation directions as a function of density. ◇ and ◆: data for samples No. 6 and No. 7.

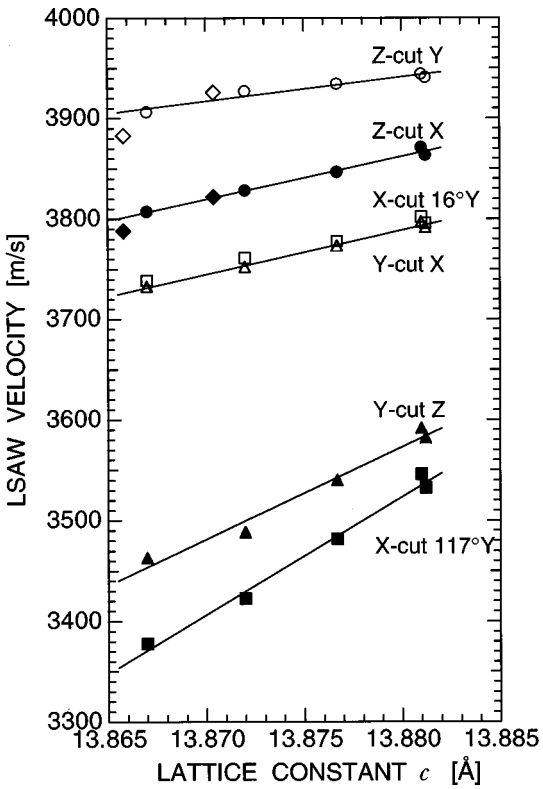

FIG. 7. LSAW velocities in typical propagation directions as a function of lattice constant *c*. ◇ and ◆: data for samples No. 6 and No. 7.

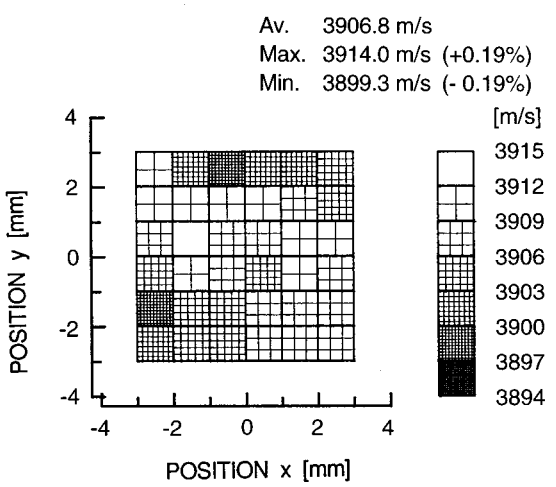

FIG. 8. Elastic inhomogeneity detection on *Z*-cut plane of specimen No. 1 for *Y*-axis propagation.

velocities decrease with the densities, so that this ultrasonic method enables us to measure local densities on the specimen surfaces, although the LSAW velocities are determined with the acoustical physical constants, including the density, associated with the propagation directions.

As the velocity increasing rates are greater on the *X*-cut planes than on the *Y*- and *Z*-cut planes, it is much better to employ the *X*-cut planes. However, in general, *Z*-cut substrates are mainly employed for optoelectronic devices, and sometimes *Y*-cut substrates are used for particular applications. The characterization must therefore be made by using the characteristic velocity information on these planes as well.

To study crystal growth conditions, velocity measurements along the crystal pulling axis, and the crystal diameter axis of specimens vertically cut and prepared from a crystal boule might present accurate information on chemical compositions for evaluation.

During the experiments, some changes in velocity were found in sample No. 1, depending upon the positions on the surface. Two-dimensional velocity measurements were thus performed, for example, for the *Y*-axis propagation on the *Z*-cut plane in 1-mm steps over a scanning area of 5×5 mm shown in Fig. 8. The results exhibit a remarkable elastic inhomogeneity in which the maximum difference in LSAW velocity is as large as 14.7 m/s (0.38%). Elastic inhomogeneity was easily and clearly observed. This inhomogeneity is considered to be mainly caused by the distribution of chemical composition rates of Mg/Li/Nb, based on the data obtained above and reported previously[14,15] and to be associated with local aggregation of Mg.[12] Compositional homogeneity in MgO: $LiNbO_3$ crystals is a necessary condition for practical use.

In the above experiments, we discussed the case of the relatively greater variations of chemical compositions. We also obtained fundamental and general knowledge of the LSAW velocity variations related to the densities, lattice constants, and other physical quantities. However, for a more practical and interesting evaluation of specimens from a single crystal boule, we might have to examine chemical composition variations of much less than 0.1 mol % along the crystal diameter axis and along the crystal pulling axis. For two-oxide compound crystals such as $LiNbO_3$ and $LiTaO_3$, the interrelations among the chemical compositions, LSAW velocities, densities, and other physical quantities can be completely determined. However, for three-oxide compound crystals such as MgO: $LiNbO_3$ treated here, more detailed experiments must be conducted to clarify the contributions of atomic components of Mg, Li, and Nb to the LSAW velocity variations. This will include measuring bulk properties, as well as LSAW properties and determining the acoustical physical constants for MgO: $LiNbO_3$ crystals with different compositions. Preliminary data of bulk properties were reported for some components of the elastic, piezoelectric, and dielectric constants.[17]

V. CONCLUDING REMARKS

In this study, we applied LFB acoustic microscopy to elastic investigation of MgO: $LiNbO_3$ single crystals to obtain basic information of the relationship of the acoustic properties, characterized by the LSAW velocities, to the chemical compositions of Mg/Li/Nb, densities, and lattice constants. Our purpose was to establish an LFB system and experimental procedure for evaluating large-diameter crystals for optical use in the growing process conditions. LSAW velocities for five MgO:$LiNbO_3$ specimens with MgO concentrations from 0 to 13 mol %, resulting in the different composition ratios of Mg/Li/Nb, were measured at 225 MHz, and the interrelations among them were determined. The LSAW velocities vary almost linearly with the MgO contents for all the surfaces and all the propagation directions. They are inversely proportional to the densities and linearly proportional to the lattice constants a and c. These results mean that it is possible to analyze and evaluate the distributions of chemical compositions or local densities by measuring the LSAW velocities using an LFB system.

The ultrasonic method can be the most useful and fundamental analytical technology, since elastic homogeneity primarily means compositional homogeneity, which is essential for obtaining high-quality MgO:$LiNbO_3$ crystals with optical homogeneity. By applying the system to evaluate a series of crystals such that Gramaier and Otto grew and studied,[10] we can determine the congruent compositions for three-oxide compounds of $MgO/Li_2O/Nb_2O_5$and the growth conditions. Significant variations of the acoustical physical constants should be accompanied by variations of the chemical compositions.[17] The precise determination of the constants associated with the needed different composition ratios of Mg/Li/Nb especially around 5-mol % MgO dopants from the industrial point of view, is highly desired as basic information for understanding the relationship between the LSAW and the bulk properties.

ACKNOWLEDGMENTS

The authors would like to thank J. L. Liu, Institute of Acoustics, Beijing, People's Republic of China, for providing the crystals; I. Sahashi and T. Sasamata, Yamaju Ceramics Co., Ltd., Seto., Japan, for providing the wafers; K. Ma-

suda, Simazu Co., Ltd., Kyoto, Japan, for measuring the chemical compositions by sequential plasma spectrometry; and T. Kikuchi, Rigaku Co., Ltd., Tokyo, Japan, for measuring the lattice constants by x-ray analysis using the Bond method. This work was supported in part by Research Grant-in-Aids from the Ministry of Education, Science, and Culture of Japan, the Toyota Physical and Chemical Research Institute, and the Murata Science Foundation.

[1] A. A. Ballman, J. Am. Ceram. Soc. **48**, 112 (1965).
[2] K. Nassau, H. J. Levinstein, and G. M. Loiacono, J. Phys. Chem. Solids **27**, 983 (1966).
[3] K. Nassau, H. J. Levinstein, and G. M. Loiacono, J. Phys. Chem. Solids **27**, 989 (1966).
[4] J. R. Carruthers, G. E. Peterson, and M. Grasso, J. Appl. Phys. **42**, 1846 (1971).
[5] G. G. Zhong, J. Jin, and Z. K. Wu, Proceedings of the 11th International Quantum Electronics, IEEE Cat. No. 80CH1561-0, 631 (1980).
[6] T. R. Volk, N. M. Rubina, V. I. Pryalkin, V. V. Krasnikov, and V. V. Volkov, Ferroelectrics **109**, 345 (1990).
[7] T. R. Volk and N. M. Rubinina, Ferroelectr. Lett. Sect. **14**, 37 (1992).
[8] Y. Kong, J. Wen, and H. Wang, Appl. Phys. Lett. **66**, 280 (1995).
[9] D. A. Bryan, R. R. Rice, R. Gerson, H. E. Tomaschke, K. L. Sweeney, and L. E. Halliburton, Opt. Eng. (Bellingham) **24**, 138 (1985).
[10] B. C. Grabmaier and F. Otto, J. Cryst. Growth **79**, 682 (1986).
[11] G. E. Peterson and S. R. Lunt, Ferroelectrics **75**, 99 (1987).
[12] Y. Furukawa, M. Sato, F. Nitanda, and K. Ito, J. Cryst. Growth **99**, 832 (1990).
[13] J. Kushibiki and N. Chubachi, IEEE Trans. Sonics Ultrason. **SU-32**, 189 (1985).
[14] J. Kushibiki, H. Takahashi, T. Kobayashi, and N. Chubachi, Appl. Phys. Lett. **58**, 2622 (1991).
[15] J. Kushibiki, T. Kobayashi, H. Ishiji, and N. Chubachi, Appl. Phys. Lett. **61**, 2164 (1992).
[16] T. Kobayashi, J. Kushibiki, and N. Chubachi, 1992 IEEE Ultrasonics Symposium Proceedings, IEEE Cat No. 92CH3118-7, 719 (1992).
[17] B. C. Grabmaier, W. Wersing, and W. Koestler, J. Cryst. Growth **110**, 339 (1991).